

November 10, 1976

ANL-FRA-TM-90

Monte Carlo Treatment of Fundamental-Mode Leakage
in the Presence of Voids

Ely M. Gelbard and Richard Leil

*Applied Physics Division
Argonne National Laboratory
Argonne, Illinois 60439*

FRA TECHNICAL MEMORANDUM NO. 90

Results reported in the FRA-TM series of memoranda frequently are preliminary and subject to revision. Consequently they should not be quoted or referenced without the author's permission.

PROPERTY OF
ARGONNE NATIONAL LAB
IDAHO LIBRARY

Work supported by the U. S. Energy Research and Development Administration.

F. W. THALGOTT - Idaho 774

The facilities of Argonne National Laboratory are owned by the United States Government. Under the terms of a contract (W-31-109-Eng-38) between the U. S. Energy Research and Development Administration, Argonne Universities Association and The University of Chicago, the University employs the staff and operates the Laboratory in accordance with policies and programs formulated, approved and reviewed by the Association.

MEMBERS OF ARGONNE UNIVERSITIES ASSOCIATION

The University of Arizona	Kansas State University	The Ohio State University
Carnegie-Mellon University	The University of Kansas	Ohio University
Case Western Reserve University	Loyola University	The Pennsylvania State University
The University of Chicago	Marquette University	Purdue University
University of Cincinnati	Michigan State University	Saint Louis University
Illinois Institute of Technology	The University of Michigan	Southern Illinois University
University of Illinois	University of Minnesota	The University of Texas at Austin
Indiana University	University of Missouri	Washington University
Iowa State University	Northwestern University	Wayne State University
The University of Iowa	University of Notre Dame	The University of Wisconsin

NOTICE

This report was prepared as an account of work sponsored by the United States Government. Neither the United States nor the United States Energy Research and Development Administration, nor any of their employees, nor any of their contractors, subcontractors, or their employees, makes any warranty, express or implied, or assumes any legal liability or responsibility for the accuracy, completeness or usefulness of any information, apparatus, product or process disclosed, or represents that its use would not infringe privately-owned rights. Mention of commercial products, their manufacturers, or their suppliers in this publication does not imply or connote approval or disapproval of the product by Argonne National Laboratory or the U. S. Energy Research and Development Administration.

Monte Carlo Treatment of Fundamental-Mode Leakage
in the Presence of Voids*

Ely M. Gelbard and Richard Lell

*Applied Physics Division
Argonne National Laboratory
Argonne, Illinois 60439*

ABSTRACT

A Monte Carlo method has been developed for the computation of the eigenvalue, as a function of buckling, in an infinite lattice. This method has been used to test the accuracy of earlier, approximate, void-worth computations, computations which enter into the analysis of hypothetical accidents in which voids collapse. Test results indicate that reactivity effects due to the collapse of bubbles in a molten pool can be computed, with reasonable accuracy by the Behrens method, used earlier by Goldsmith. On the other hand, Webb's estimates of eigenvalue changes, caused by the expansion of fuel pins into the voids of a previously voided lattice, appear to be somewhat too high.

*Work supported by the U. S. Energy Research and Development Administration.

I. INTRODUCTION

Prescriptions for the treatment of streaming effects in practical reactor computations are based, generally, on numerous approximations, approximations which are often not easy to assess. As a result it is impossible to determine, a priori, how accurately computations, based on such prescriptions, will predict neutronic properties of some particular reactor. Under such circumstances, extensive testing is required to establish the validity of the various techniques available for use in streaming calculations.

Tests of the accuracy of computational methods fall into two, qualitatively different classes. In one class we find tests against experiment, tests in which computational and experimental results are compared. In the other are tests of all sorts in which the results of approximate computations are compared with "exact" results, i.e. computational results which are known to be so accurate that, in practice, we may regard them as exact.

In the literature on streaming and anisotropic diffusion we find, however, that definitive test results of any kind are scarce. Those tests which have been carried out are generally tests of the Benoist method. Benoist¹ has made extensive comparisons between Benoist-method computations (with and without absorption corrections) and various experimental data. These comparisons suggest that the Benoist method is quite useful, but give little information, directly, on its accuracy or limitations. Much more impressive evidence of the validity of Benoist's method has come out of the analysis of recent SNEAK experiments at Karlsruhe.² In these experiments sodium void worths were measured as functions of the height of the

sodium-void interface. This was done in each of two configurations, one with horizontal and one with vertical plates. Differences between worths in those configurations were substantial, yet the worths were given quite accurately by the Benoist method (apparently without absorption corrections).

While such experimental confirmation is essential, experimental tests of streaming computations have very severe limitations. First, the net amount of experimental information available to us is small, and is likely to remain small, since experimental data on streaming are very expensive. Secondly, comparisons with experiment are inevitably ambiguous because of uncertainties in our cross section libraries. It seems clear, therefore, that high-precision benchmark computations must play a most important role in testing the various approximate techniques designed for streaming computations.

Yet there are in the literature very few purely computational tests of the adequacy of any such techniques. Thus, for example, we find only one case in which the Benoist method is tested against a high-precision benchmark calculation. This test is discussed in a recent paper by Kobayashi, et al.³ Here the authors take, as their benchmark configuration, a very simple two-zone reactor in r-z geometry. Each of the two zones (representing, respectively, a core and a blanket) is composed of a lattice of horizontal-plate cells, a lattice which extends to infinity along the z axis. Via one-group S_n calculations, the authors compute an eigenvalue and flux shape in their benchmark reactor with the lattice represented explicitly. They then recalculate the eigenvalue and flux shape by diffusion theory, using a fairly conventional version of the Benoist method. In this case, the authors conclude, the Benoist method works very well.

But the use of S_n codes to test approximate streaming computations is only practical in one- or simple two-dimensional geometries. Transport calculations in complicated three-dimensional geometries require Monte Carlo codes. To compute, by Monte Carlo, small eigenvalue differences between explicit and homogenized reactor configurations would, generally, be very expensive: many histories would be required to raise these differences above the statistical noise. We find, however, that Monte Carlo studies of anisotropic streaming effects are perfectly feasible if one is willing to retain some restrictions on the problem geometry. It is our main purpose, here, to show that this is true. Below we shall develop specialized techniques for benchmark streaming calculations in lattices. These techniques may be applied to lattices with very complicated cells, but we will always assume that the lattice itself is infinite and uniform. Leakage effects will be introduced through bucklings, and we shall compute the lattice eigenvalues as functions of these bucklings. Such an approach, obviously, has serious weaknesses in that it tells us nothing about streaming effects near boundaries of a real, finite lattice. On the other hand, a benchmark calculation of eigenvalues as a function of buckling provides us with the most direct (and, conceptually, the simplest) check on the validity of anisotropic diffusion approximations. These approximations almost invariably assume the presence of a well-defined buckling. Therefore, it seems natural to ask, first of all, how well they approximate the lattice eigenvalue when a buckling really does exist.

Our Monte Carlo estimate of lattice eigenvalues will be based on a very simple relation, derived by perturbation theory. We develop this relation next, in Section II, and then digress briefly to draw some inferences from it. Finally, in Section III, we apply our Monte Carlo method to lattice configurations of two different types, both containing voids.

II. FUNDAMENTAL RELATION FOR THE LATTICE EIGENVALUE AS A FUNCTION OF BUCKLING

Suppose the fission spectrum is the same for all nuclides and is independent of the energy of the absorbed neutron. This is an assumption which we will make in our derivation below and one which may be justifiable, in different circumstances, for different reasons. First, the use of a single fission spectrum is often a good approximation, especially in reactors where most fissions occur in one particular nuclide. But, secondly, we can if we like enforce, in our test problems, an artificially imposed restriction that all nuclides have one and the same fission spectrum. This might be done simply to guarantee the validity of benchmark calculations designed to test some approximate computational method. In our multi-energy test calculations, however, we have taken cross sections and fission spectra directly from ENDF/B-III, and our assumption that there is only one fission spectrum for all nuclides must be viewed as an approximation.

Making this approximation, it becomes possible in any infinite lattice to define a fission Green's function, $G(\underline{r}' \rightarrow \underline{r})$, which has a very simple meaning: $G(\underline{r}' \rightarrow \underline{r}) d\underline{r}$ is the number of fissions produced, per second, in $d\underline{r}$, by one fission per second at \underline{r}' . It is crucial to our argument that this number of fissions be independent of the flux spectrum at \underline{r}' .

In the absence of leakage (i.e. at $\underline{B} = 0$), the lattice eigenvalue problem takes the form

$$k_0 s_0(\underline{r}) = \int G(\underline{r}' \rightarrow \underline{r}) s_0(\underline{r}') d\underline{r}' , \quad (1)$$

where $s_0(\underline{r})$ has the periodicity of the lattice. Now suppose there is a well-defined buckling in the lattice. Suppose, in fact, that there are well-defined x, y, and z bucklings so that we may write

$$s(\underline{r}) = \mathcal{R} \{ s(\underline{r}) e^{i\mathbf{B} \cdot \underline{r}} \}, \quad (2)$$

where, now $s(\underline{r})$ is periodic (and generally complex). In the presence of these bucklings

$$\left. \begin{aligned} kS(\underline{r}) &= \int G(\underline{r}' \rightarrow \underline{r}) S(\underline{r}') d\underline{r}', \\ \text{or} \\ kS(\underline{r}) &= \int G(\underline{r}' \rightarrow \underline{r}) e^{i\mathbf{B} \cdot (\underline{r}' - \underline{r})} s(\underline{r}') d\underline{r}' \end{aligned} \right\} \quad (3)$$

It will be seen that, if \mathbf{B} is very small, Eqs. (1) and (3) are integral equations with very slightly different kernels. Therefore, by perturbation theory,

$$\Delta k \equiv k_0 - k \approx \frac{\int s_0^*(\underline{r}) d\underline{r} \int G(\underline{r}' \rightarrow \underline{r}) \left[1 - e^{i\mathbf{B} \cdot (\underline{r}' - \underline{r})} \right] s_0(\underline{r}') d\underline{r}'}{\int s_0^*(\underline{r}) s_0(\underline{r}) d\underline{r}}, \quad (4)$$

where s_0^* is the adjoint fission source, such that

$$k_0 s_0^*(\underline{r}) = \int G(\underline{r} \rightarrow \underline{r}') s_0^*(\underline{r}') d\underline{r}'.$$

From Eq. (4)

$$\frac{\Delta k}{k_0} \approx \frac{\int s_0^*(\underline{r}) d\underline{r} \int G(\underline{r}' \rightarrow \underline{r}) \left[1 - e^{i\mathbf{B} \cdot (\underline{r}' - \underline{r})} \right] s_0(\underline{r}') d\underline{r}'}{\int s_0^*(\underline{r}) d\underline{r} \int G(\underline{r}' \rightarrow \underline{r}) s_0(\underline{r}') d\underline{r}'} \quad (5)$$

If the unit cell has three orthogonal symmetry planes, the imaginary part of Δk will vanish:

$$\frac{\Delta k}{k_0} \approx \tau \equiv \frac{\int s_0^*(\underline{r}) \, d\underline{r} \int G(\underline{r}' \rightarrow \underline{r}) [1 - \cos \underline{B} \cdot (\underline{r}' - \underline{r})] s_0(\underline{r}') \, d\underline{r}'}{\int s_0^*(\underline{r}) \, d\underline{r} \int G(\underline{r}' \rightarrow \underline{r}) s_0(\underline{r}') \, d\underline{r}'} \quad (6)$$

It is this last equation, Eq. (6), which we will use as the basis for our Monte Carlo calculations.

There are, of course, many different Monte Carlo methods which could be used to estimate the right-hand side of Eq. (6). Assume, for the moment, that we know the adjoint fission source, $s_0^*(\underline{r})$. Then we might, for example, proceed as follows. We would, first, run an ordinary, generation-by-generation, Monte Carlo eigenvalue calculation, random-walking histories through the lattice. In the course of this calculation, records would be kept of the location, \underline{r}' , at which each particle was born, and the point, \underline{r} , at which it was absorbed. For each sample neutron we would compute

$$\xi_i \equiv \frac{s_0^*(\underline{r}_i) [1 - \cos \underline{B} \cdot (\underline{r}'_i - \underline{r}_i)] v_{\Sigma f}(\underline{r}_i)}{\Sigma_a(\underline{r}_i)}, \quad i = 1, 2, \dots, N. \quad (7)$$

Here N is the total number of sample neutrons, and the index, i , identifies individual histories. Further \underline{r}'_i is the birth location of the i -th sample neutron, while \underline{r}_i is the point at which it was absorbed. It seems reasonable to expect that

$$\xi \equiv \frac{\sum_{i=1}^N \xi_i}{\sum_{i=1}^N \left[s_0^*(\underline{r}_i) v_{\Sigma f}(\underline{r}_i) / \Sigma_a(\underline{r}_i) \right]} \approx \tau. \quad (8)$$

More precisely, it seems clear that, as the number of generations, and the number of histories per generation, tend to infinity, the estimator ξ will converge in probability to τ .

If τ , as defined by Eq. (6), can be expanded in powers of the components of \underline{B} then, to lowest order in these components,

$$\frac{\Delta k}{k} = \frac{1}{2} \left[\overline{B_x^2 \ell^2} + \overline{B_y^2 \ell^2} + \overline{B_z^2 \ell^2} \right], \quad (9)$$

$$\overline{\ell^2}_{x,y,z} \equiv \frac{\int s_0^*(\underline{r}) \, d\underline{r} \int G(\underline{r}' \rightarrow \underline{r}) (r'_{x,y,z} - r_{x,y,z})^2 s_0(\underline{r}') \, d\underline{r}'}{\int s_0^*(\underline{r}) \, d\underline{r} \int G(\underline{r}' \rightarrow \underline{r}) s_0(\underline{r}') \, d\underline{r}'}$$

It will be seen that the quantities $\overline{\ell^2}_{x,y,z}$ are mean-square distances from birth to fission, weighted by the adjoint fission source at each fission site. Again, to leading order

$$k = k_0 / \left[1 + \frac{1}{2} \left(\overline{\ell^2 B_x^2} + \overline{\ell^2 B_y^2} + \overline{\ell^2 B_z^2} \right) \right]. \quad (10)$$

Equation (10) generalizes to lattices the relation

$$k = k_0 / [1 + M^2 B^2], \quad M^2 = \frac{1}{6} \overline{\ell^2}, \quad (11)$$

valid for homogeneous media.

To use the method described above one needs to know the adjoint fission source, s_0^* . This is a disadvantage of the proposed method but, generally, it is not a very serious disadvantage. The adjoint source in a cell (i.e. the importance function for fission) is usually pretty flat, and it is often permissible to assume that it is constant. We find, in fact, in two test cases discussed below, that s_0^* really is constant.

When necessary, it is often possible (as has been pointed out by Matthes⁴) to calculate s_0^* in the course of the Monte Carlo calculation which generates s_0 . This could be done, for example, as follows:

1. Subdivide all fuel-bearing regions into boxes. These should be small enough so that s_0 is nearly flat over each box, but large enough so that, in each box, a reasonable number of histories will start and end.
2. Compute the number of fission neutrons produced in box j , at the end of each generation, by sample neutrons which started that generation in box i . From this information form the Green's function for fission, $G(i \rightarrow j)$.
3. Transpose the Green's function and solve the adjoint eigenvalue problem.

From Eq. (10), in one-group problems, we can easily define an effective homogenized diffusion coefficient:

$$D_{x,y,z} = \frac{1}{2} \bar{\Sigma}_a \bar{\ell}_{x,y,z}^2.$$

Here $\bar{\Sigma}_a$ is the cell-averaged absorption cross section, weighted with the zero-buckling scalar flux. Further $\bar{\ell}_x^2$, $\bar{\ell}_y^2$, and $\bar{\ell}_z^2$ are mean-square distances from birth to fission, weighted with the importance function s_0^* . It is interesting to note that the Benoist method (without absorption corrections) gives a result formally identical with Eq. (10): but in the Benoist version the mean-square distances are unweighted averages of squares of distances from birth to absorption. It is in part due to these differences that the Benoist method does not preserve the lattice eigenvalue,⁵ even in one-group problems.

We have assumed, so far, that the lattice cell has three orthogonal symmetry planes: but what if it does not? In this case we must expect that Δk , as defined by Eq. (6), will generally be complex. When this is true then, strictly speaking, a buckling cannot exist anywhere in the lattice.

If a reactor core is composed of such a lattice a buckling will not exist anywhere in the core.

Note that Δk is always real in one-group problems, regardless of the cell geometry. (This assertion is proven in Appendix A.) It is easy, however, to construct a multigroup problem configuration in which Δk is complex, so that there can be no buckling. We consider, for example, a two-group model of a slab reactor composed of asymmetric cells. The cell geometry is shown in Fig. 1, and cell parameters are listed in Table I. Our slab reactor consists of 40 such cells, side by side, with vacuum boundaries on the left- and right-hand faces of the slab. We have computed the flux in this reactor by diffusion theory, but a transport solution would not be qualitatively different. The thermal flux is plotted in Fig. 2. It will be seen that this flux (and, of course, the fission source) is strongly asymmetric. Obviously the curve in Fig. 2 looks nothing like a cosine, and we find that one cannot fit a cosine very well to any segment of this curve (any reasonably long segment) anywhere within the core.

Much of the theory of homogenization is based on the assumption that the fission source is separable, as in Eq. (2). The assumption implies that the fission source within the lattice has, roughly, a cosine shape. The global cosine shape is, however, slightly corrugated; that is, it is distorted by the local bumps and dips induced by local structure in each lattice cell. A priori it seems no more implausible to make such an assumption than to postulate a cosine fission source in any simple homogeneous material, and in fact we will continue to assume a buckling in all the work reported here. Nevertheless, as we have seen, this is not always an admissible assumption. Clearly it makes little sense to postulate a buckling in a reactor whose structure is sufficiently irregular. Apparently a buckling cannot exist, strictly

speaking, even in perfect lattice, if the lattice cell is asymmetric. In fact, little has been done, so far, to establish a range over which Eq. (2) is valid, although the concept of a buckling in a lattice plays a fundamental role in many reactor computations. Clearly, much work is needed before we can establish where we have the right to introduce a buckling. To define homogenized cross sections, and homogenized diffusion coefficients, without assuming any buckling is rather difficult. The problem of homogenizing a reactor's small-scale structure without relying on a buckling is discussed extensively in Ref. 6.

It seems appropriate, before closing this section, to comment on the accuracy and range of validity of the proposed perturbation method. Clearly Eqs. (9) and (10) are only accurate to second order in the components of \underline{B} . Further, these equations are not valid, for any range of bucklings, unless the mean-square chord lengths, $\overline{\ell_x^2}$, $\overline{\ell_y^2}$, and $\overline{\ell_z^2}$, are all finite. In practice it is not at all safe to assume that either of these conditions will be satisfied.

Thus, for example, it is not unusual for leakage probabilities in fast reactors (particularly in GCFRs, or sodium-voided LMFBRs) to reach 30%. In situations of this sort it would certainly be rash to assume that B^4 terms in Δk can be neglected, or that Eqs. (9) and (10) are interchangeable.

Neither is it unusual to find that two, or all three, of the mean-square path lengths are infinite. In fact, as has been pointed out by Köhler and Ligou,⁷ if a lattice contains planar regions which are entirely void at least two of the mean-square path lengths must be infinite. Of course, planar voids will always occur in a slab lattice, or a square

lattice of fuel pins, if the coolant is voided. But a voided hexagonal lattice will also contain planar voids⁷ if the void fraction is, roughly, greater than 32%.

The range of validity of Eq. (6) is determined by quite different considerations. First of all we have not required, in deriving this equation, that any mean-square chord length be finite. In our derivation we have treated leakage as a perturbation and thus, implicitly, we have assumed that $(\Delta k/k_0) \ll 1$: but there are situations where even this assumption is unnecessary. After all, Eq. (6) would be exact if we replaced s_0^* , the unperturbed adjoint source, by s^* , the adjoint source perturbed by the buckling. But suppose a cell contains only one fuel pin, or plate, and that this pin or plate is very small in mean-free paths. Then the adjoint source will be almost flat, and remain almost flat even when the leakage probability is large. Correspondingly, even when $(\Delta k/k_0) \approx 1$, Eq. (6) may be a good approximation. In fact, it is interesting to note that Eq. (6) is rigorous for any buckling if the cell is homogeneous.

III. APPLICATIONS

In this section we apply the methods developed above to two void streaming problems. These problems have been chosen for inclusion, here, not because of their intrinsic importance, but because we feel they serve us very well as illustrative examples. Both problem configurations are fairly simple, but three-dimensional. Both problems have already been treated approximately by other authors. In both problems void streaming is singled out as the only significant effect.

We begin with a discussion of a problem first posed and analyzed by R. E. Webb in a thesis written at Ohio State University.⁸ Webb postulates an LMFBR accident in which sodium has been expelled from the core. Further, the clad has melted, so that bare fuel pins are surrounded by void. At this point the fuel expands and uniformly fills each cell. Homogenization decreases leakage from the lattice, increasing the lattice eigenvalue. Through one-group calculations Webb estimates the eigenvalue change produced by this smearing of fuel in the Fermi and EBR-II reactors. His one-group lattice parameters are listed in Table II. We shall not attempt to decide whether these parameters are reasonable or not but it should be noted that the fuel pins in Webb's model are only, roughly, a tenth of a mean-free path in diameter. One may expect, therefore, that even for rather high bucklings, the adjoint source will remain fairly flat and our perturbation method will continue to be valid. Later we shall try to show that perturbation theory in this case is, in fact, quite accurate.

Webb's computations are based on the Behrens method,⁹ drastically modified to accommodate peculiar features of the voided lattices. The formulas developed by Behrens, for the treatment of streaming through holes, contain a factor, Q , which depends on the shape of the holes. In lattices containing planar voids Q is always infinite,¹⁰ and planar voids occur in all the voided lattices Webb treated in his thesis. Webb notes, however, that the divergence of integrals defining Q results from artificial features of idealized lattices (which, by definition are, of course, perfectly regular and infinitely large). To avoid such divergent integrals, Webb attempts to apply the Behrens method to finite lattices, and to define a range of plausible Q values for finite Fermi and EBR-II cores. We shall not review

his reasoning here, but simply exhibit his final results. Webb's estimated eigenvalue changes, computed via his modified Behrens method, are listed in the first row of Table III.

Corresponding eigenvalue changes have also been computed by Monte Carlo processes like those discussed above in Section II. Note that if a lattice is composed of one, single material, then no matter how the density of that material varies in a cell, the unperturbed adjoint source, s_0^* , is flat. Thus, in this case s_0^* drops out of Eq. (6).

Our Monte Carlo results appear, along with Webb's, in Table III. It will be seen that Webb's reactivities are substantially higher than ours but are, in order of magnitude, quite reasonable.¹¹

So far our computations have all been based on perturbation theory. It is interesting to note, however, that if \underline{B} is purely axial, the exact equation for the lattice eigenvalue takes a very simple form, a most convenient form for Monte Carlo simulation. To develop an effective Monte Carlo simulation method, we assume, again, that

$$kS(\underline{r}) = \int G(\underline{r}' \rightarrow \underline{r}) S(\underline{r}') d\underline{r}', \quad (12)$$

using the same notation as in Eq. (2). Now we postulate that $S(\underline{r}) = s(x,y) \cos Bz$, and find that

$$\begin{aligned} ks(x,y) &= \int G(x',y',z' \rightarrow x,y,z) s(x',y') \cos B(z' - z) d\underline{r}' \\ &= \int G[x',y',0 \rightarrow x,y,(z - z')] s(x',y') \cos B(z' - z) d\underline{r}'. \end{aligned} \quad (13)$$

Apparently Eq. (13) was first obtained by Köhler and Ligou and we have, here, followed their derivation closely. It will be convenient, in Eq. (13), to let $Z = z' - z$, so that

$$ks(x,y) = \int G(x',y',0 \rightarrow x,y,Z) s(x',y') \cos(BZ) dx' dy' dZ. \quad (14)$$

We evaluate k from Eq. (14) by a conventional iterative process, starting from a guessed fission source. Drawing sample neutrons from this source (always with $z = 0$), we random-walk these neutrons through a single generation, producing fission source sites by conventional techniques. We then multiply the weight attached to each source site by $\cos BZ$, where Z is the vertical coordinate of that site. The modified weights are then used, next, to establish a source distribution for the beginning of the second generation. The whole process is then repeated, this time taking sample neutrons from the new source distribution.

In principle, of course, it is possible to reiterate this process indefinitely. In practice, however, one finds that the particle weights will fluctuate more and more in succeeding generations, and that more and more weights will turn negative. Eventually, the whole Monte Carlo process becomes hopelessly inefficient as the variance within generations tends to infinity. This deterioration progresses at a rate which increases with $|B|$. Fortunately the convergence rate of our iterative process in cell problems will, generally, be very high (if the cell is not too large in mean-free paths). The convergence rate of a Monte Carlo process depends, roughly, on the dominance ratio, δ ,¹² defined as the ratio of the first two eigenvalues, $\delta \equiv k_2/k_1$. Here k_1 is the dominant eigenvalue, while k_2 corresponds to the first overtone. In our case the entire Monte Carlo calculation is carried out within a single cell; the first overtone fission source will change sign within the cell, on some curve in the x, y plane, so that the radial buckling will be very high and, correspondingly, k_2 will be low. We can expect, as a result, that $\delta \ll 1$, and, thus, that convergence will be very fast.

In Table IV we list estimates of the quantity $\Delta k/k$ computed by Monte Carlo, for the EBR-II lattice. Here

$$\Delta k/k \equiv \left[k_{\text{HOM}}(\underline{B}) - k_{\text{HET}}(\underline{B}) \right] / k_{\text{HET}}(\underline{B}), \quad (15)$$

where k_{HET} is the eigenvalue in the original, heterogeneous lattice, while k_{HOM} is the eigenvalue in the homogenized lattice.¹³ Cross sections in the homogeneous cell are obtained, of course, by volume-averaging those in the heterogeneous cell.

The entries in Table IV correspond, as will be seen, to two different bucklings. The first buckling ($B^2 = 0.00204$) is just the Z buckling in Webb's EBR-II calculations. The second ($B^2 = 0.00564$) is the net buckling in Webb's calculations treated, here in our calculation, as if it were all in the Z direction.

In both cases the initial Monte Carlo fission source was flat. It is easy to show that the eigenvalue obtained at the end of the first generation is exactly the same as the perturbation theory eigenvalue defined by Eq. (6). A flux dip at the surface of the fuel pin, induced by leakage should develop in the second and succeeding generations, raising the heterogeneous eigenvalue, $k_{\text{HET}}(\underline{B})$, and thus lowering $\Delta k/k$. Apparently, however, this shift in eigenvalue is too small to be observed here. It seems safe to say that our initial results, shown in Table III, are accurate to within the indicated statistical uncertainties.

We now turn to a second accident scenario, discussed in another Ohio State University publication, a Master's thesis by Goldsmith.^{15,16} Goldsmith assumes that a core meltdown has occurred for some reason, and that molten fuel is lying, in a bubbling pool, on the floor of the reactor vessel. One would expect that, as the temperature rises in the pool, the Doppler effect

would come into play, limiting the total energy released in the excursion. But this process takes a finite time, during which perhaps the pressure in the pool may rise to such a point as to collapse the bubbles. Goldsmith postulates that all the bubbles collapse simultaneously and so quickly that the volume-averaged density of fuel remains unchanged.

We shall not ask here whether such a sequence of events is plausible. There are various reasons for skepticism but, at any rate, bubbles may appear in molten fuel, and one ought to be able to determine their worth. In his thesis Goldsmith, like Webb, computes void worths by the Behrens method. However, since Q is finite in this case, the Behrens method may be used directly without difficulty. Further, the use of the Behrens method is justifiable, here, if one is willing to accept a very simple model of the boiling pool. To see in what sense this is true, we review key steps in Goldsmith's argument.

In his reactivity computations, Goldsmith postulates, first of all, that the eigenvalue is given by the following equations:

$$k(B^2) = k_0 / (1 + M^2 B^2),$$

$$k_0 \equiv v \Sigma_f / \Sigma_a, \quad M^2 = \frac{1}{6} \overline{\ell^2}. \quad (16)$$

Here $\overline{\ell^2}$ is the mean-square distance a neutron travels from birth to absorption. Thus, in the original bubble-filled pool

$$k_{\text{HET}} = k_0 / \left(1 + \frac{1}{6} \overline{\ell_{\text{HET}}^2} B^2 \right), \quad (17)$$

and, after collapse of the bubbles

$$k_{\text{HOM}} = k_0 / \left(1 + \frac{1}{6} \overline{\ell_{\text{HOM}}^2} B^2 \right). \quad (18)$$

Clearly Eqs. (17) and (18) imply that there is a well-defined buckling in the pool, and that this buckling does not change when the bubbles collapse. Further it has been assumed, here, that the physical properties of the fuel-bubble mixture are uniform, at least over much of the pool. Combining Eqs. (17) and (18) we find that

$$\Delta \equiv k_{\text{HOM}} - k_{\text{HET}} = \frac{(k_0 - k_{\text{HOM}})}{k_0} \left[\frac{\bar{\ell}_{\text{HET}}^2}{\bar{\ell}_{\text{HOM}}^2} - 1 \right]. \quad (19)$$

Finally, assuming $k_{\text{HOM}} \approx 1$, Goldsmith writes

$$\Delta = \frac{(k_0 - 1)}{k_0} \left[\frac{\bar{\ell}_{\text{HET}}^2}{\bar{\ell}_{\text{HOM}}^2} - 1 \right] \equiv \frac{(k_0 - 1)}{k_0} \rho, \quad (20)$$

$$\rho \equiv \left[\frac{\bar{\ell}_{\text{HET}}^2}{\bar{\ell}_{\text{HOM}}^2} - 1 \right].$$

Before any further discussion of Goldsmith's computations, it is necessary to comment, briefly, on his definition of $\bar{\ell}^2$. Goldsmith explicitly takes $\bar{\ell}^2$ to be the mean-square distance from birth to absorption. But it is easy to show that, in our one-group problem configuration, the mean-square distances to absorption and fission are the same. Thus, the mean-square distance to fission, given any source, $S(\underline{r})$, and weight function $w(\underline{r})$, is given by the expression

$$\bar{\ell}_f^2 = \frac{\int w(\underline{r}) d\underline{r} \int G(\underline{r}' \rightarrow \underline{r}) |\underline{r}' - \underline{r}|^2 S(\underline{r}') d\underline{r}'}{\int w(\underline{r}) d\underline{r} \int G(\underline{r}' \rightarrow \underline{r}) S(\underline{r}') d\underline{r}'}.$$

The mean-square distance to absorption is

$$\bar{\ell}_a^2 = \frac{\int w(\underline{r}) \left[\Sigma_a(\underline{r}) / \nu \Sigma_f(\underline{r}) \right] \int G(\underline{r}' \rightarrow \underline{r}) |\underline{r}' - \underline{r}|^2 S(\underline{r}') d\underline{r}'}{\int w(\underline{r}) \left[\Sigma_a(\underline{r}) / \nu \Sigma_f(\underline{r}) \right] \int G(\underline{r}' \rightarrow \underline{r}) S(\underline{r}') d\underline{r}'}$$

Clearly, so long as the ratio $\Sigma_a / \nu \Sigma_f$ is position-independent, $\bar{\ell}_f^2 = \bar{\ell}_a^2$.

We have the right, then, to consider Goldsmith's mean-square distances as mean-square distances to fission, and it will be convenient to do so in our work below.

It has already been shown above that Eq. (17) is valid, to first-order in B^2 , for regular lattices: Goldsmith, however, uses this same expression to treat bubbles which are randomly arranged. To generalize our arguments so as to deal with such arrays is not at all a simple matter.¹⁷ It should be noted that even our definition of buckling is only applicable to periodic lattices. Of course, we cannot expect that bubbles in a molten pool will place themselves on lattice sites of any kind but, if there are enough bubbles in the pool, exact details of their arrangement may be unimportant. The bubbles could then be rearranged in many ways without changing the eigenvalue in the pool. Imagine, for example, that the bubbles are rearranged by the following process.

First the whole pool is divided into cubes, all equal in size. Each cube is to be large enough to contain many bubbles, yet small enough so that many cubes fit into the pool. Next one cube is selected (a "typical" cube) and that cube is used, in place of all the others, to construct a second, replica pool which (aside from details of the bubble distribution) is just like the first. If there are enough bubbles in the pool, and in the typical cube, then (barring unlikely accidental bubble configurations) we may expect that the original and replica pools will have almost equal

eigenvalues. If this is true, we have successfully replaced an irregular array of bubbles with a bubble lattice, and we can now write

$$k(\underline{B}) = k_0 / \left(1 + \frac{1}{6} \overline{\lambda^2 B^2} \right). \quad (21)$$

Of course in principle the $\overline{\lambda^2}$ in Eq. (26) should be computed in the bubble lattice, not in the random bubble array. In practice, however, we shall neglect this fine distinction: $\overline{\lambda^2}$ in our computations (as in Goldsmith's) will be the mean-square distance from birth to fission in the original random array. It seems reasonable to expect, nevertheless, that Eq. (21) will give a useful estimate of the effect of random features in the bubble distribution.

Now, assuming the validity of Eq. (21) we proceed to test the accuracy of Goldsmith's mean-square path-length computation. These mean-squares are computed, in Goldsmith's work, by the Behrens method.⁹ But it has been pointed out by Benoist¹ that the Behrens method is generally incorrect in that Behrens neglects angle-path-length correlations between successive flights. Such correlations exist in heterogeneous media even when the scattering is isotropic.¹ Behrens assumes, in other words, that

$$\overline{\lambda^2} = \bar{n} \overline{\lambda_1^2}. \quad (22)$$

Here $\overline{\lambda_1^2}$ is the mean-square length of a single free-flight, while \bar{n} is the mean number of flights per neutron history. Equation (22) is incorrect in general:¹ one can show, however, that it is correct, in one group, whenever Σ_s/Σ_t and $v\Sigma_f/\Sigma_t$ are position independent.¹⁸

In summary, then, we find that Eq. (17) is correct for low bucklings and regular bubble lattices. Further, it seems reasonable to use Eq. (17)

to treat random arrangements of bubbles. The mean-square distance in Eq. (22) is equal to the mean-square length of each flight, times the mean number of flights per neutron history. In this sense the Behrens method is valid.

On the other hand, other aspects of this method remain to be discussed. Thus, to assess Goldsmith's results, it will be necessary to test the accuracy of the Behrens formulas used by Goldsmith to compute the mean-square lengths of single flights. We have done this by simple Monte Carlo methods.

Our Monte Carlo computations were carried out for regular bubble lattices, and for irregular bubble arrays: but we did not attempt, in any of our work, to deal with "truly random" arrays. In fact it is not clear at all what is meant by a "random" array of bubbles. This term has been used here rather loosely to designate a bubble distribution which contains irregularities of some sort. One would certainly expect irregularities in a network of bubbles formed in molten fuel. It is also possible, however, that systematic features will be forced onto the bubble distribution by laws which govern the nucleation, growth, and motion of the bubbles.¹⁹ Since so little is known about the nature of the "random" bubble distributions, the effort required to generate and store such distributions seems to be unwarranted. Instead we have run Monte Carlo calculations for "randomized" arrays, constructed as follows:

Imagine the molten fuel cut up into cells, all identical in size and shape. Suppose, for convenience, that these cells are cubes, as they are in all the work discussed below. Suppose, further, that the bubbles are perfectly spherical. Select a cell width, a bubble diameter (smaller than or equal to this width), and a probability, p , that any given cell contains

a bubble. Then, in each cell independently, decide by random sampling methods whether that specific cell contains a bubble; or does not.²⁰ If there is a bubble in the cell then, as in the regular arrays, it is placed exactly at the center of the cube. It will be seen that the "randomized" arrays, as constructed here, have both regular and random features, tending to become more regular as $p \rightarrow 1$.

In Table V we list some values of the quantity ρ , $\rho \equiv \left(\frac{\overline{\ell}_{\text{HET}}^2}{\overline{\ell}_{\text{HOM}}^2} \right) - 1$,²¹ computed for various bubble arrays, by various methods.¹⁴ Here $\overline{\ell}_{\text{HOM}}^2$ and $\overline{\ell}_{\text{HET}}^2$ are, respectively, mean-square path lengths in "corresponding" homogeneous and heterogeneous media, i.e. homogeneous and heterogeneous media with equal average densities. In all cases cited in this table the bubbles were taken to be spheres with $d = 2$ cm, where d is the bubble diameter. In each case the bubble volume constituted 25% of all the volume of the liquid-bubble mixture; but the total cross section of pool material (i.e. the material around the bubbles) varied in our computations, covering a range from 0.1 to 4 cm^{-1} . Regular and irregular arrays differed, primarily, in t , the thickness of the cubic cell.

With d given in regular arrays, the cell width is determined by the bubble volume fraction. When this fraction is 25%, we find, still assuming $d = 2$, that $t \approx 2.56$ cm. On the other hand, in randomized arrays there is, at our disposal, an additional degree of freedom: t , in such arrays, is determined jointly by the bubble volume fraction and by the probability p . Now we have already noted that the "randomized" arrays become more regular as p increases. Therefore, in all our calculations, we take p as small as possible for a given volume fraction. It is easy to see that p is minimized when t and d are equal, so that a bubble just barely fits into a cell. Given that $t = d$, it turns out that we must set $p = 0.477$ to achieve a bubble volume fraction in the randomized array of 25%.

Values of ρ , computed by the Behrens method, are listed in columns 2 and 3 of Table V, and corresponding Monte Carlo values will be found in columns 4 and 5. The confidence intervals in columns 4 and 5 are standard deviations.

Behrens, in his first paper on void streaming,⁹ actually gives three different approximate expressions for $\overline{\ell^2}$. One is designed to treat widely spaced holes, while a second is specifically for closely spaced holes. The third (the Behrens "general" formula) interpolates between the other two, asymptotically approaching the appropriate limits as the bubble spacing goes to zero and infinity. It will be seen that, over the whole range of our table, the Monte Carlo ρ values agree fairly well with ρ values computed through use of the prescription for closely-spaced holes. The general formula, on the other hand, gives poor results when λ , the mean free path, is large. It is interesting to note that Goldsmith, in all his thesis work, used only the formula for closely spaced holes. We will not discuss here his arguments for this procedure: in fact, his logic is not entirely consistent with our computational results. At any rate, whatever the reason, Goldsmith's choice of the formula for closely spaced holes was apparently correct.

It will be seen from Table V that, given λ , $\overline{\ell^2}$ is greater for randomized arrays than for regular lattices. This effect is probably due to the occurrence of bubble clusters in the randomized arrays. Apparently the formation of such clusters more than compensates for the blockage of long streaming paths which are present in the regular lattice, but are closed off by fluctuations in the randomized bubble pattern.

We see that, for regular lattices, the Behrens closely spaced hole formula generally overestimates ρ , but is accurate here to within about 20%.

For our randomized lattices this same formula underestimates ρ , though not by more than 10%. At low bucklings (and within the limitations of Goldsmith's model) a 10% error in ρ produces a 10% error in Δ [see Eq. (20)]: the numbers listed in Table V gives us, then, a clear indication of the accuracy of Goldsmith's results. But, of course, as the leakage probability approaches unity, one cannot any longer neglect B^4 and higher-order terms in k . These terms may have a significant effect on the bubble reactivity, and we examine this effect next.

If, at the buckling of the pool, the fission source and the adjoint source are practically flat, then, from Eq. (6),

$$\frac{\Delta k}{k_0} = \frac{\int d\underline{r} \int G(\underline{r}' \rightarrow \underline{r}) [1 - \cos \underline{B} \cdot (\underline{r}' - \underline{r})] d\underline{r}'}{\int d\underline{r} \int G(\underline{r}' \rightarrow \underline{r}) d\underline{r}'} , \quad (23)$$

$$\equiv \frac{1}{(1 - \cos \underline{B} \cdot \Delta \underline{r})} \equiv R .$$

Using the above equation, in place of Eq. (11), in Goldsmith's derivation, we get

$$\Delta = \frac{\hat{\rho}(k_0 - 1)}{k_0} , \quad \hat{\rho} = \left[\frac{R_{\text{HET}}(1 - R_{\text{HOM}})}{R_{\text{HOM}}(1 - R_{\text{HET}})} - 1 \right] . \quad (24)$$

It will be seen that Eqs. (20) and (24) are formally the same but that here, in Eq. (24) $\hat{\rho}$ takes the place of ρ .

Clearly Δ , as defined in Eq. (24), depends on the buckling B^2 . The buckling, in turn, will depend on the size and the shape of the pool and thus, implicitly, on the entire history of the accident. Since one can postulate many different accident scenarios it seems impossible to single out a buckling here by any very rigorous argument. Instead we shall try

to select a plausible buckling and, for that buckling, will then compute $\hat{\rho}$.

Suppose that, in a DEMO plant, the sodium is voided and a meltdown occurs. Reasonable number densities for the liquid in the molten pool (i.e. the material around the bubbles) are listed in Table VI.¹⁴ In Table IX we have also listed corresponding one-group constants computed for a pool made of this liquid, but with a void fraction of 25%.¹⁴

Unless the molten pool is close to critical, we must expect that neutron streaming in the bubbles will not be crucially important. Therefore, as in Eq. (20) we assume that k (k_{HOM} , for convenience) is 1.0. In a one-group model, with parameters taken from Table IX, we find that this pool will just be critical when $B^2 = 0.0037$. Monte Carlo values of ρ and $\hat{\rho}$ computed at this buckling, still in the same one-group model, are listed in Table VII. There, for comparison, we also list ρ values computed by the Behrens method for closely spaced holes. We see some indication, in Table VII, that transport effects do reduce the bubble reactivities, but such effects, if they exist, are too small to be treated, reliably, by any of the methods discussed in our paper. From all the data listed here in Tables V and VII, we conclude that Goldsmith's bubble reactivities are reasonably accurate even for the bucklings postulated in the molten pool.

IV. DISCUSSION

Obviously many questions about the Webb and Goldsmith calculations remain unanswered. The models used by Webb and Goldsmith, models we have adopted also in our benchmark calculations, are grossly oversimplified. Some approximations in these models are rigidly built into our computational techniques. Thus our Monte Carlo calculations are firmly based on the assumption that a

well-defined buckling exists in the lattice. On the other hand, it is not difficult in Webb's fuel pin computations to drop the single-group approximation and redo these calculations with a full-scale, multi-energy, Monte Carlo code.

Today calculations of void worths in the Fermi and EBR-II reactors seem somewhat dated. For this reason we have chosen not to redo the original Webb calculations but, instead, to compute a multienergy void worth in a simplified DEMO plant cell geometry. This computation was carried out with the aid of a version of VIM,¹² specially modified for our purposes by R. Prael. Parameters characterizing the problem configuration are listed in Table VIII. We find, in this case, that homogenization of the rods increases the lattice eigenvalue by $\approx 0.005 \pm 0.0006$.¹⁴ This effect is of the same order of magnitude as those studied earlier in one-group calculations.

It has still been assumed in this calculation, as in all the work reported here, that the buckling does not change when the voids disappear. This may not really be true for various reasons. Obviously if the homogenization process is accompanied by other changes in the core geometry, the buckling will probably also change. But even if no other changes in geometry occur, homogenization alone may change the buckling. The buckling in a reactor core will, after all, depend on the extrapolation length at the core-blanket, or core-reflector interface. There is some reason to believe¹⁴ that this extrapolation length will drop substantially if, in the voided lattice, the pins are homogenized. Such an effect would tend, to some extent, to decrease the resulting reactivity insertion. Very little is known at this time about flux shapes near interfaces in voided lattices and we cannot, therefore, predict the magnitude of this effect with any confidence.

The bubble worth calculation has also been repeated, for one regular cubical bubble lattice, with the aid of the same modified version of VIM. Parameters which characterize the molten pool were taken, again, from Table VI. We recall that all parameters in this table are thought to typify a pool which might be formed in the meltdown of a DEMO plant. In a pool with these parameters the eigenvalue change which is produced when we homogenize the pool is $\approx 0.011 \pm 0.001$. In the corresponding one-group calculation we get, instead, an eigenvalue change $\approx 0.014 \pm 0.002$. It is not difficult to see why one-group calculations might overestimate the worth of voids. All our one-group constants were obtained by flux-weighting: our one-group Σ_t is, thus, a flux-weighted average of $\Sigma_t(E)$. But the leakage will tend to be relatively high where Σ_t is relatively small. Thus a flux weighted average Σ_t may well exaggerate the magnitude of all effects induced by leakage from the lattice.

S_n bubble-worth calculations have been run by MacLaughlin and Turner²² at Los Alamos. The problem configurations discussed in Ref. 22 and here, in our work, are very different from each other: it is impossible, therefore, to make detailed comparisons between our results and those reported from Los Alamos. Roughly, however, their results agree with Goldsmith's and with ours.

In Goldsmith's work, as in Ref. 22 there is some discussion of streaming effects which we have not dealt with here explicitly. There are, in fact, two such effects, namely:

- (1) the "mass importance effect"; and
- (2) the "neutron self-multiplying effect".

Apparently the first effect, as envisioned by Goldsmith, would occur in a molten pool if bubbles were denser near its center than near its

outer boundary. This density difference might come about accidentally, as a result of statistical fluctuations in the bubble distribution.

It seems clear that we cannot deal with fluctuations of this sort in our calculations, which make no distinctions between one part of the pool and another. Goldsmith finds this mass importance effect to be small, and we have no way to confirm or refute this conclusion.

A somewhat different "mass importance effect" has been discussed, more recently by McLaughlin.²³ In this latest work, McLaughlin feeds void reactivities directly into hydrodynamics calculations, and computes fuel distributions as a function of time throughout the course of a postulated accident. According to the computations reported by McLaughlin, a net outward flow of fuel accompanies the pressure pulse which tends to close the bubbles. The author finds that the decrease in importance of the fuel as it moves outward compensates, almost exactly, for the reactivity inserted by the collapse of bubbles. Again, this sort of "mass importance effect" cannot be included in our work.

On the other hand, the neutron self-multiplying effect, first noted by McLaughlin and Turner, can be treated by methods used above, in our bubble computations. The effect itself is easily understood. Suppose, for example, that very tiny bubbles, uniformly scattered, compose half the volume of the pool. The diffusion coefficient, D , in the pool is then equal to two thirds Σ_t . Here Σ_t is the total cross section of the liquid in the pool, the liquid between the bubbles. Now suppose that f , the bubble volume fraction, remains constant, while the bubble radius gradually increases. Then D , at first, will also increase because of streaming effects. But if the bubble growth continues, the distances between the bubbles will finally far exceed the mean-free path λ , where $\lambda \equiv 1/\Sigma_t$. At

this point, the liquid between bubbles will act like an infinite multiplying, homogeneous medium with $D = 1/3 \Sigma_t$. Thus, there must come a time when the effective D stops increasing but, instead, moves downward towards a limit half as large as its initial value. For convenience we have used a one-group terminology in this discussion but our argument is, in fact, perfectly general.

As the bubble size increases the mean-square path length becomes infinite. We draw this conclusion, for example, from the properties of Behrens' widely-spaced hole formula. Thus, the Behrens method would give us an infinite diffusion coefficient for infinitely large bubbles, and it is for this reason that MacLaughlin separates the "Behrens effect" from the neutron "self-multiplying effect".

Suppose, however, that we compute the eigenvalue in the pool through use of Eq. (6), taking note of the fact that, in this case s_0 and s_0^* are flat. Imagine the pool to be divided into two sets of zones. Pool material lying in zones of the first set ("A zones") is located within, let us say, 100 mean-free-paths of the surface of a bubble, while material in the other set of zones ("B zones") is not. As the bubble size increases (with f constant) most of the fuel will come to lie in B zones, while relatively less and less remains in A zones. But for all the tracks which start in A zones the average $[1 - \cos \underline{B \cdot \Delta r}]$ is finite. Therefore, τ , defined in Eq. (6) will eventually reach the same limit as if there were no bubbles in the pool. In this sense, the self-multiplying effect is contained in Eq. (6).

On the other hand, as the bubble size increases, s^* will eventually start to dip near bubble surfaces. Since, in our work, this dip has been ignored, our bubble reactivities for small λ 's (perhaps for $\lambda = 0.25$ in Table V) may be too large.

It has been our purpose, here, to develop a high-precision Monte Carlo method for benchmark streaming calculations. We hope this method will prove useful, eventually, for testing design and analysis techniques in realistic situations. Here, however, we have focussed our attention on relatively simple illustrative examples so as to bring out salient features of our method as sharply as possible.

The strong and weak points of this method should be fairly clear by now. We impose a buckling, or several bucklings simultaneously, in a Monte Carlo calculation. The bucklings need not be established by outer iteration, as in more common Monte Carlo processes. Further the buckling need not be deduced from the Monte Carlo output but is instead, part of the input. In short, we feel the proposed method is an efficient and convenient technique for computing eigenvalues, as functions of buckling, in complicated lattices.

As for its disadvantages, one which we have mentioned earlier seems most important. Our method cannot treat interlattice boundaries, boundaries between regions with different lattice structure. Benchmark computations in the presence of such boundaries would be extremely difficult by any available technique. For relatively simple geometries such computations are possible by S_n methods as Kobayashi and his coworkers have shown.³ But more realistic reactor configurations with explicit lattice structure are likely to be three-dimensional. S_n calculations in such configurations would be extremely expensive, and perhaps totally unfeasible at this time. Our inability to treat boundaries between lattices in high-precision streaming computations seems a serious weakness in present computational techniques.

Appendix A

VANISHING OF THE IMAGINARY PART OF THE ONE-GROUP EIGENVALUE

In one group we can always write

$$kS(\underline{r}) = \int G(\underline{r}' \rightarrow \underline{r}) S(\underline{r}') d\underline{r}', \quad (\text{A-1})$$

where G is the fission Green's function and S is the fission source.

Since $S = v\Sigma_f \phi$:

$$kv\Sigma_f(\underline{r})\phi(\underline{r}) = \int G_\phi(\underline{r}' \rightarrow \underline{r}) v\Sigma_f(\underline{r}) v\Sigma_f(\underline{r}') \phi(\underline{r}') d\underline{r}', \quad (\text{A-2})$$

Here G_ϕ is the flux Green's function, i.e. the scalar flux at \underline{r} due to an isotropic delta function source at \underline{r}' . From Eq. (A-2) we see that

$$\begin{aligned} k\psi(\underline{r}) &= \int \hat{G}(\underline{r}' \rightarrow \underline{r}) \psi(\underline{r}') d\underline{r}', \\ \psi(\underline{r}) &\equiv \sqrt{v\Sigma_f(\underline{r})} \phi(\underline{r}), \\ \hat{G}(\underline{r}' \rightarrow \underline{r}) &\equiv \sqrt{v\Sigma_f(\underline{r}')} G_\phi(\underline{r}' \rightarrow \underline{r}) \sqrt{v\Sigma_f(\underline{r})}. \end{aligned} \quad (\text{A-3})$$

Since G_ϕ is symmetric, \hat{G} is also symmetric, and k must be real.

Further one can show that $\hat{\tau}$,

$$\hat{\tau} \equiv \frac{\int s_0^*(\underline{r}) d\underline{r} \int G(\underline{r}' \rightarrow \underline{r}) [1 - e^{iB \cdot (\underline{r}' - \underline{r})}] s_0(\underline{r}') d\underline{r}'}{\int s_0^*(\underline{r}) s_0(\underline{r}) d\underline{r}}, \quad (\text{A-4})$$

the perturbation theory estimate of Δk , is also real. To show that this is true we examine the adjoint integral equation. By definition

$$k s_0^*(\underline{r}) = \int G(\underline{r} \rightarrow \underline{r}') s_0^*(\underline{r}') d\underline{r}', \quad (\text{A-5})$$

or

$$k s_0^*(\underline{r}) = \int G_\phi(\underline{r} \rightarrow \underline{r}') v\Sigma_f(\underline{r}') s_0^*(\underline{r}') d\underline{r}',$$

$$k s_0^*(\underline{r}) = \int G_\phi(\underline{r}' \rightarrow \underline{r}) v_{\Sigma_f}(\underline{r}') s_0^*(\underline{r}') d\underline{r}' . \quad (A-6)$$

But

$$k \phi_0(\underline{r}) = \int G_\phi(\underline{r}' \rightarrow \underline{r}) v_{\Sigma_f}(\underline{r}') \phi_0(\underline{r}') d\underline{r}' . \quad (A-7)$$

On comparing Eqs. (A-6) and (A-7) we see that $s_0^* = \phi_0$, so that

$$\hat{\tau} = \frac{\iint d\underline{r} d\underline{r}' H(\underline{r}', \underline{r}) [1 - e^{i\underline{B} \cdot (\underline{r}' - \underline{r})}]}{\int s_0^*(\underline{r}) s_0(\underline{r}) d\underline{r}} , \quad (A-8)$$

$$H(\underline{r}', \underline{r}) \equiv v_{\Sigma_f}(\underline{r}') \phi_0(\underline{r}') G_\phi(\underline{r}' \rightarrow \underline{r}) v_{\Sigma_f}(\underline{r}) \phi_0(\underline{r}) .$$

Since H is symmetric in \underline{r}' and \underline{r} , the imaginary part of $\hat{\tau}$ must vanish.

Appendix B

EIGENVALUE AS A FUNCTION OF B IN AN INFINITE RANDOM ARRAY OF BUBBLES

Consider an infinite medium containing a "random" array of bubbles. Suppose there is a finite (even though small) probability that a tremendous cube cut out of this medium, a cube perhaps 100 mean-free paths in width, contains no bubbles. Then somewhere in the medium there will be just such a bubble-free cube. But this cube is, itself, essentially infinite and the behavior of neutrons within the cube will be almost unaffected by the distribution of bubbles around it. Suppose the fission source, deep in the cube, has a cosine distribution with buckling B^2 . Then the only possible eigenvalue for the whole infinite medium is the infinite medium eigenvalue in the absence of bubbles, for the given buckling B^2 . Thus the concept of an infinite, "random" array of bubbles seems not very useful unless the bubble distribution is severely constrained.

Appendix C

ABSENCE OF FLIGHT-TO-FLIGHT CORRELATION IN THE ONE-GROUP BUBBLE CALCULATION

Consider an infinite diffusing medium which, in a one-group model, has the property that

$$\frac{\Sigma_s(\underline{r})}{\nu\Sigma_f(\underline{r})} = \text{const.} = \alpha. \quad (\text{C-1})$$

Within our very simple model the flux throughout the medium is governed by the following equation:

$$\hat{\Omega} \cdot \nabla F + \Sigma_t F = \frac{1}{2} \nu\Sigma_f \left[\alpha + \frac{1}{\lambda} \right] \phi. \quad (\text{C-2})$$

where λ is the system eigenvalue. If, now, we set $\Sigma_s(\underline{r}) = 0$, without altering Σ_t or $\nu\Sigma_f$, the transport equation takes on the new form

$$\Omega \cdot \nabla F_a + \Sigma_t F_a = \frac{1}{2} \frac{\nu\Sigma_f}{\lambda_a} \phi_a. \quad (\text{C-3})$$

On comparing Eqs. (C-2) and (C-3), it is easy to see that, in fact,

$$F = F_a, \quad \phi = \phi_a, \quad (\text{C-4})$$

and

$$\frac{1}{\lambda_a} = \alpha + \frac{1}{\lambda} = \frac{\Sigma_s}{\nu\Sigma_f} + \frac{1}{\lambda}. \quad (\text{C-5})$$

If the medium is a lattice then, at very low bucklings

$$\lambda = \frac{v\Sigma_f}{\Sigma_a} \left/ \left(1 + \frac{1}{2} \ell^2 B^2 \right) \right., \quad \lambda_a = \frac{v\Sigma_f}{\Sigma_t} \left/ \left(1 + \frac{1}{2} \ell_1^2 B^2 \right) \right., \quad (C-6)$$

$$\frac{\ell^2}{\ell_1^2} = \left(\frac{v\Sigma_f/\Sigma_a}{\lambda} - 1 \right) \left/ \left(\frac{v\Sigma_f/\Sigma_t}{\lambda_a} - 1 \right) \right. . \quad (C-7)$$

But, from Eq. (C-5)

$$\frac{v\Sigma_f/\Sigma_t}{\lambda_a} = \frac{\Sigma_s}{\Sigma_t} + \frac{v\Sigma_f/\Sigma_t}{\lambda} = 1 - \frac{\Sigma_a}{\Sigma_t} + \frac{\Sigma_a}{\Sigma_t} \frac{v\Sigma_f/\Sigma_a}{\lambda} , \quad (C-8)$$

$$\frac{v\Sigma_f/\Sigma_t}{\lambda_a} - 1 = \frac{\Sigma_a}{\Sigma_t} \left(\frac{v\Sigma_f/\Sigma_a}{\lambda} - 1 \right) , \quad (C-9)$$

so that

$$\ell^2 = \bar{n} \ell_1^2 , \quad \bar{n} = \frac{\Sigma_t}{\Sigma_a} , \quad (C-10)$$

as in Eq. (23) of the text.

REFERENCES

1. P. BENOIST, "Theorie due Coefficient de Diffusion dans un Réseau Comportant des Cavités," Centre d'Etudes Nucléaires-Saclay Rep. CEA-R-2278 (1964).
2. E. A. FISCHER, et al., "An Investigation of the Heterogeneity Effect in Sodium Void Reactivity Measurements," in *Proc. Intern. Symp. on Physics of Fast Reactors*, Tokyo, Japan, October 16-19, 1973, Vol. II, pp. 945-963.
3. T. KOBAYASHI, et al., *J. Nucl. Sci. Techn. (Tokyo)*, 12, 456 (1975). See also T. YOSHIDA and S. IIJIMA, *J. Nucl. Sci. Techn. (Tokyo)*, 13, 161 (1976). This paper appeared in print after our own article had been accepted for publication. For this reason it is not discussed in our text.
4. W. MATTHES, *Nucl. Sci. Eng.*, 47, 234 (1972).
5. E. M. GELBARD, *Nucl. Sci. Eng.*, 54, 327 (1974).
6. A. HENRY, *Nuclear Reactor Analysis*, MIT Press, Cambridge, Mass. (1975).
7. P. KÖHLER and J. LIGOU, "Axial Streaming Problem in Gas-Cooled Fast Reactors," EIR-244 (1973).
8. R. E. WEBB, "Some Autocatalytic Effects During Explosive Power Transients in Liquid Metal-Cooled, Fast Breeder, Nuclear Power Reactors (LMFBRs)," Ph.D. Dissertation, The Ohio State University (1971).
9. D. J. BEHRENS, *Phys. Soc. London Proceedings, Sec. A*, 62, 607 (1949).
10. In such cases the Benoist D is also infinite, so that Webb's lattice cannot be treated rigorously by the Benoist method.
11. In computing the reactivities reported here, we have used radial and axial bucklings taken from Webb's thesis. However, on repeating

- Webb's buckling calculations as best we can, we get bucklings (for both Fermi and EBR-II) which are about half as large as Webb's.
12. E. M. GELBARD and R. E. PRAEL, "Monte Carlo Work at Argonne National Laboratory," in *Proc. NEACRP Meeting of a Monte Carlo Study Group*, July 1-3, 1974, Argonne, Illinois, U.S.A., Argonne National Laboratory Rep. ANL-75-2 (1975), pp. 202-233.
 13. To minimize variance, the homogeneous and heterogeneous eigenvalues were computed simultaneously. For details of the computational technique, see Ref. 14.
 14. R. M. LELL, "Neutron Streaming and Anisotropic Diffusion in Partially Voided Lattices," Ph.D. Dissertation, The Ohio State University (1976).
 15. G. L. GOLDSMITH, "Reactivity Due to Neutron Streaming in the Voids of a Bubbly Pool Core," M.S. Thesis, The Ohio State University (1974).
 16. R. B. NICHOLSON, "Design Basis Accident Studies: Final Report," C00-2286-3, Part Five (1974).
 17. We show in Appendix B that, in attempting to generalize Eq. (22) rigorously to random bubble arrays, one encounters serious fundamental difficulties.
 18. See Appendix C. In Ref. 1 Benoist has essentially derived Eq. (25) for a lattice of widely spaced holes in an otherwise homogeneous medium. It will be seen that our results in Appendix C include Benoist's, but are somewhat more general.
 19. E. G. SCHLECHTENDAHL, "Sieden des Kühlmittels in Natriumgekühlten Schnellen Reaktoren," Karlsruhe Rep. KFK-1020 (1969).
 20. Note that it is not really necessary to preassign and store the location of each bubble. Through the use of delta scattering it is possible in this particular problem configuration to decide after a collision is made in a cell whether or not that cell contains a bubble.

21. It should be noted that Goldsmith's bubble reactivities, as defined by Eq. (25) are proportional to ρ .
22. T. P. McLAUGHLIN and G. D. TURNER, "Reactivity Changes Due to Bubble Growth or Collapse in Molten Fuel Systems," *Trans. Am. Nucl. Soc.*, 21, 281 (1975).
23. T. P. McLAUGHLIN, "Effects of Neutron Streaming and Geometric Models on Molten Fuel Reactivity Recriticality accidents," Los Alamos Scientific Laboratory, LA-6127-MS (1975).

TABLE I
Asymmetric Lattice Cell Cross Sections

Moderator		Absorber		Fuel	
Group 1	Group 2	Group 1	Group 2	Group 1	Group 2
$\Sigma_{a1} = 0$	$\Sigma_{a2} = 0.2$	$\Sigma_{a1} = 0$	$\Sigma_{a2} = 10$	$\Sigma_{a1} = 0$	$\Sigma_{a2} = 10$
$\nu\Sigma_{f1} = 0$	$\nu\Sigma_{f2} = 0$	$\nu\Sigma_{f1} = 0$	$\nu\Sigma_{f2} = 0$	$\nu\Sigma_{f1} = 0$	$\nu\Sigma_{f2} = 10$
$\Sigma_{t1} = 1.01$	$\Sigma_{t2} = 1$	$\Sigma_{t1} = 0$	$\Sigma_{t2} = 10$	$\Sigma_{t1} = 0$	$\Sigma_{t2} = 10$
$\Sigma_{1-1} = 0.01$	$\Sigma_{2-2} = 0.8$	$\Sigma_{1-1} = 0$	$\Sigma_{2-2} = 0$	$\Sigma_{1-1} = 0$	$\Sigma_{2-2} = 0$
$x_1 = 1$	$\Sigma_{1-2} = 1.0$		$\Sigma_{1-2} = 0$		$\Sigma_{1-2} = 0$
	$x_2 = 0$	$x_1 = 1$	$x_2 = 0$	$x_1 = 1$	$x_2 = 0$

TABLE II

Webb's Reactor Parameters and One-Group Cross Sections

	EBR-II	Fermi
Basic Lattice Cell		
Geometry	Hexagonal	Square
Width of cell across flats, cm	0.584	0.56007
Radius of fuel pins, cm	0.183	0.175
Buckling, cm^{-2}		
Radial	36.0×10^{-4}	17.8×10^{-4}
Axial	20.4×10^{-4}	10.3×10^{-4}
Σ_a , cm^{-1} (solid fuel)	0.0427	0.0357
$\nu\Sigma_f$, cm^{-1} (solid fuel)	0.0858	0.0643
Σ_t , cm^{-1} (solid fuel)	0.325	0.325
Σ_s , cm^{-1} (solid fuel)	0.2823	0.2893
L_0^2 (solid fuel), cm^2	24.0	28.7

TABLE III

One-Group Reactivity Estimates for EBR-II and Fermi

	$\Delta k/k$ (%)	
	EBR-II	Fermi
Webb	0.9-1.7	0.9-1.7
Monte Carlo	0.63 ± 0.063	0.84 ± 0.084

TABLE IV

Iteration and Perturbation Estimates of $\Delta k/k$ for EBR-II^{*}

	$\Delta k/k$	
	$B^2 = 20.4 \times 10^{-2}$	$B^2 = 56.4 \times 10^{-4}$
Iteration	0.001256 ± 0.000037	0.001507 ± 0.000091
Perturbation	0.001165 ± 0.00012	0.001440 ± 0.00015

* Note that the values of $\Delta k/k$ listed here are computed as if the pin material were a pure absorber.

TABLE V
Heterogeneity Effect for Bubbles

λ	$\left(\overline{\lambda_{het}^2} / \overline{\lambda_{hom}^2} \right) - 1$			
	Behrens		Monte Carlo	
	Closely Spaced	General	Regular Cube	Random Cube
0.25	0.5625	0.5	0.5074 ± 0.0018	0.6038 ± 0.0022
0.5	0.2813	0.2189	0.2454 ± 0.0012	0.3057 ± 0.0014
1	0.1406	0.0828	0.1206 ± 0.0009	0.1544 ± 0.0030
2	0.0703	0.0274	0.0586 ± 0.0007	0.0787 ± 0.0007
3	0.0469	0.0142	0.0396 ± 0.0006	0.0521 ± 0.0006
4	0.0352	0.0030	0.0292 ± 0.0006	0.0390 ± 0.0006
5	0.0281	0.0064	0.0240 ± 0.0005	0.0322 ± 0.0006
7	0.0201	0.0039	0.0180 ± 0.0005	0.0221 ± 0.0005
10	0.0141	0.0024	0.0116 ± 0.0005	0.0157 ± 0.0005

Note: $\left(\overline{\lambda_{het}^2} / \overline{\lambda_{hom}^2} \right) - 1$ for $f = 0.25$, $d = 2$ cm.

Here λ is the mean-free path in the material between bubbles.

TABLE VI
Geometry Parameters and Composition
for Bubble Lattice Cell

Lattice array	Regular cubic array
Bubble radius, cm	0.793701 cm
Side of cube, cm	2.030982 cm
Void fraction	0.25
$B^2(B_x = B_y = B_z)$	0.003733
Cross sections	ENDF/B level 3
Composition of fuel prior to fuel expansion:	
<u>Isotope</u>	<u>No. Density (atoms/cm³)</u>
²⁴⁰ Pu	0.66736×10^{21}
²⁴¹ Pu	0.34960×10^{21}
²³⁵ U	0.10622×10^{21}
²³⁸ U	0.15134×10^{23}
²³⁹ Pu	0.23490×10^{22}
Cr	0.14189×10^{22}
Ni	0.96939×10^{21}
Fe	0.37448×10^{22}
¹⁶ O	0.37448×10^{23}
Mo	0.10985×10^{21}
⁵⁵ Mn	0.13429×10^{21}
k_{∞}	1.5719 ± 0.0031

TABLE VII

 ρ and $\hat{\rho}$ for $\lambda = 0.25, 3, 10$ with $d = 2$ cm and $f = 0.25$

λ	ρ			$\hat{\rho}$	
	Behrens C. S.	M. C. Regular	M. C. Random	M. C. Regular	M. C. Random
0.25	0.5625	0.5074 ± 0.0018	0.6038 ± 0.0022	0.4908 ± 0.015	0.6064 ± 0.020
3.0	0.0469	0.0396 ± 0.0006	0.0521 ± 0.0006	0.0375 ± 0.0062	0.0404 ± 0.0061
10.0	0.0141	0.0116 ± 0.0005	0.0157 ± 0.0005	0.0078 ± 0.0042	0.0131 ± 0.0043

TABLE VIII

Geometry Parameters and Composition for CRBR Cell

Lattice cell	Hexagonal
Pin radius, cm	0.2921
Side of hexagonal cell, cm	0.4194103
Equivalent outer cylinder radius, cm	0.38140826
Void fraction	0.41348
B_r^2 , cm^{-2}	4.8997×10^{-4}
B_z^2 , cm^{-2}	4.6942×10^{-4}
Cross sections	ENDF/B level 3
Composition of intact pin -- fuel and clad homogenized together in pin:	
<u>Isotope</u>	<u>No. Density (atoms/cm³)</u>
²⁴⁰ Pu	0.385845×10^{21}
²⁴¹ Pu	0.550715×10^{20}
²³⁵ U	0.802042×10^{20}
²³⁸ U	0.113890×10^{23}
²³⁹ Pu	0.285338×10^{22}
Cr	0.393535×10^{22}
Ni	0.195256×10^{22}
Fe	0.140739×10^{23}
¹⁶ O	0.289482×10^{23}
Mo	0.296944×10^{23}
k_∞	1.688 ± 0.004

TABLE IX

One-Group Macroscopic Cross Sections
for Pin and Bubble Lattices -
Intact Pins and Unexpanded Fuel

	Pin Lattice	Bubble Problem
$\nu\Sigma_f, \text{ cm}^{-1}$	0.017431	0.017596
$\Sigma_a, \text{ cm}^{-1}$	0.010147	0.011225
$\Sigma_s, \text{ cm}^{-1}$	0.353830	0.367428
$\Sigma_t, \text{ cm}^{-1}$	0.363977	0.378653

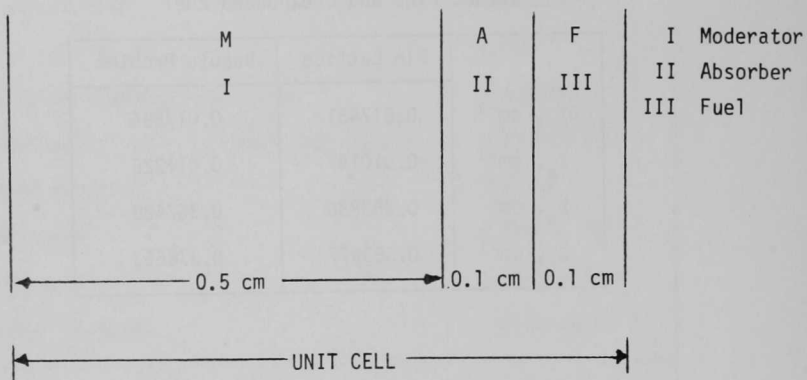


Fig. 1. Asymmetric cell geometry.

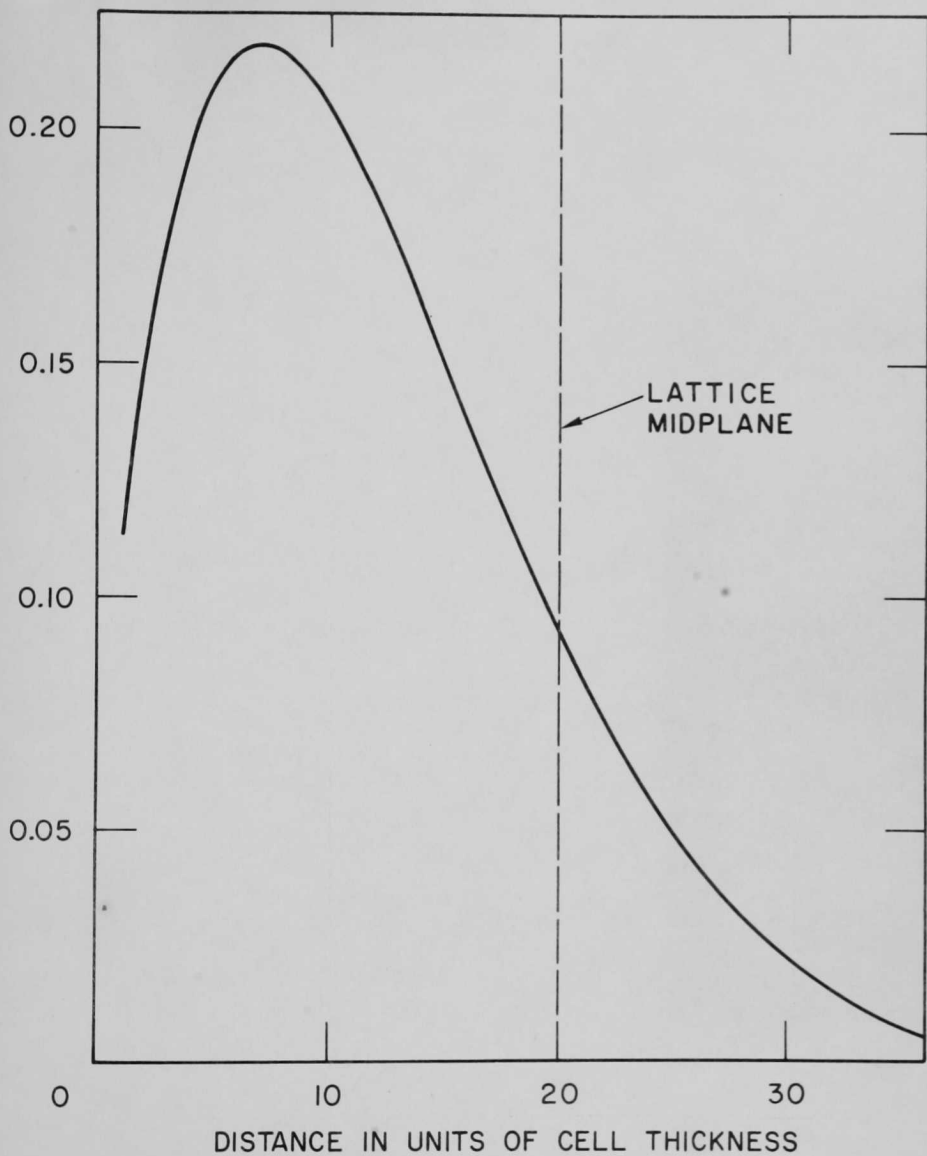


Fig. 2. Thermal flux (normalized to an integral of unity.)



2

